Resource Allocation for Hierarchical Underwater Sensor Networks

Fatemeh Fazel
Northeastern University
Boston, MA 02115
Email: ffazel@ece.neu.edu

Milica Stojanovic
Northeastern University
Boston, MA 02115
Email: millitsa@ece.neu.edu

***Abstract*—We investigate data collection over an underwater acoustic communication network, where sensor nodes are deployed to measure an environmental process. To enhance the energy-efficiency, the network is organized into a hierarchical structure, in which multiple local fusion centers collect the information and convey it to a master fusion center. The master fusion center then recovers the map of the sensing field. We exploit the unique properties of the underwater signal propagation to allocate resources efficiently across the network, resulting in overall savings in the energy and a reduction in the minimum necessary bandwidth.**

I. Introduction

In an underwater acoustic sensor network, communication bandwidth is severely constrained because of the frequency dependent signal attenuation. Hence, data collection schemes which are able to operate in low bandwidths are highly desirable. In [1], we proposed Random Access Compressed Sensing (RACS) which provides an efficient means of collecting data from a large network, where efficiency is defined in terms of the energy per bit of information successfully delivered, and the minimum bandwidth required to enable successful telemetry. To efficiently collect data from a large number of sensor nodes, wireless sensor networks are generally organized in a hierarchical structure [2]. Thus, to improve the scalability and to further enhance the energy efficiency of a RACS network, we adopt a hierarchical structure in which the network is divided into districts (clusters). Each sensor employs random sensing (i.e., senses the field at a random instants in time, with some average sensing rate) and communicates its data to the local fusion center (cluster head) over a random access channel. The local FCs then convey the gathered information to a master FC, where using all of the packets gathered collaboratively, the full map of the sensing field is reconstructed. Thus, the overall architecture is that of joint data collection by the local FCs, with centralized processing by the master FC. Employing a hierarchical structure reduces the energy consumption of a RACS network because wireless transmission occurs over shorter distances. We also show that the hierarchical structure reduces the requirements on the minimum bandwidth needed for successful field recovery, enabling the data collection to be achieved with even smaller bandwidths, which is a desirable feature for bandwidth-limited underwater networks.

The rest of the paper is organized as follows: In Section II, we introduce the network structure, briefly review signal propagation properties in an underwater channel, and determine the interference radius. Section III provides a model for the packet collection process. In Section IV, we study the bandwidth requirements of the hierarchical network. Energy consumption is studied in Section V, and optimal resource allocation is discussed in Section VI. Finally, concluding remarks are made in Section VII.

II. Hierarchical Network Structure

In wireless networks, data communication is the main source of energy consumption [3]. A hierarchical data collection approach can thus extend the network lifetime by reducing the transmission energy. Employing a hierarchical scheme, we divide a large area S_{tot} into D districts, each of radius R. Each district communicates its observations to a local FC, placed in the center of the district. The local FCs then communicate their gathered data to a master FC, which recovers the map of the field. Assuming a total of N sensor nodes covering the area S_{tot}, and a node density ρ, the number of nodes in each district is given by

$$N_0 = \frac{N}{D} = \rho \pi R^2 \tag{1}$$

Each local FC not only receives packets from the N_0 nodes in its own district, but also from the interfering nodes in the neighboring districts.[1] In order to determine the interference radius R_{int}, we first review the propagation characteristics of an underwater channel.

A. Underwater Path-Loss and Noise Models

A unique property of underwater acoustic communication is that signal attenuation increases not only with distance but also with frequency. In an underwater acoustic communication channel the path-loss over a distance r in meters is described by [4]

$$A(r, f) = A_0 r^k a(f)^r \tag{2}$$

where A_0 is the normalizing constant including fixed losses, $a(f)$ denotes the absorption coefficient that depends on the frequency f, and k denotes the spreading factor. Using Thorp's formula, the absorption loss can be expressed in dB/km as

$$10 \log_{10} a(f) = \frac{0.11 f^2}{1+f^2} + \frac{44 f^2}{4100+f^2} + \frac{2.75 f^2}{10^4} + 0.003 \tag{3}$$

where f is in kHz [4]. According to this model, path-loss increases with both distance and frequency, as is shown in Fig. 1. Throughout this paper, we use values $A_0 = 30$ dB and spreading factor $k = 1.5$.

The ambient noise in the ocean can be modeled as [4]

$$10 \log_{10} \eta(f) = \eta_0 - 18 \log_{10} f \tag{4}$$

where f is in kHz, and η_0 is a site-specific constant e.g. $\eta_0 = 50$ dB re 1 μPa^2/Hz for calm deep sea. Note that, unlike the path-loss, the noise p.s.d decays with the frequency.

B. Interference Radius

Let us define the operating spectrum as the range of frequencies $f \in [f_0, f_0 + B]$, where f_0 is called the operating frequency and B is the bandwidth. In Section VI, we will investigate how to choose the optimal operating frequency $f_0^\star$. Throughout this paper, we approximate the path-loss and the noise p.s.d by their corresponding values at f_0, i.e., we assume

$$\begin{aligned} A(r, f) &\approx A(r, f_0) \quad \forall f \in [f_0, f_0 + B] \\ \eta(f) &\approx \eta(f_0) \quad \forall f \in [f_0, f_0 + B] \end{aligned} \tag{5}$$

[1]We assume all districts use the same frequency band to communicate to their local FCs, consequently causing interference to their neighboring districts' FCs.

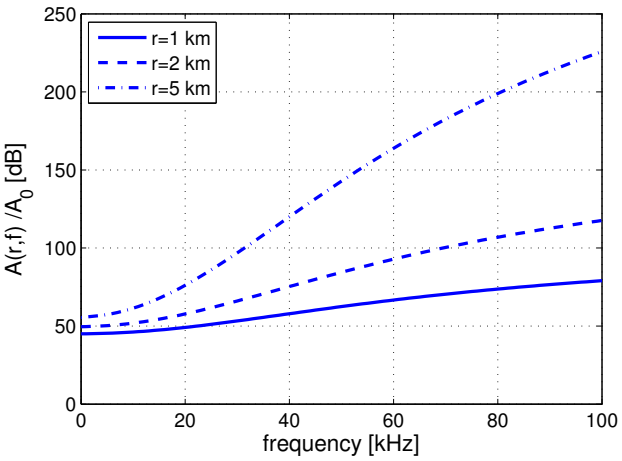

Fig. 1. Normalized path-loss $A(r, f)/A_0$ plotted vs. frequency. Path-loss increases with both distance and frequency.

The SNR for a transmission distance r and an operating frequency f_0, is given by

$$SNR(r, f_0) = \frac{P_T(r)}{A(r, f_0)\eta(f_0)B} \tag{6}$$

where $P_T(r)$ is the transmit power. Assuming that the local FC has a target received SNR denoted by γ_0, the sensor node located at a distance r from its local FC adjusts its transmission power such that its packet is received at the desired SNR γ_0, i.e.,

$$P_T(r) = \gamma_0 A(r, f_0)\eta(f_0)B \tag{7}$$

For a given local FC, transmissions from the sensor nodes within the area of radius $R_{\text{int}} > R$ can be detected by the FC. Some of these transmissions are from the nodes located within the local FC's own district (i.e., within the radius R), while others are from the neighboring districts. We assume that each FC will only collect the packets from its own district and will discard the ones originating from the neighboring districts. This is a suboptimal strategy, since the local FCs can also collect the packets from neighboring districts (within the interference region). In that case, if a packet experiences collision at its own local FC, it may still be successfully received by an adjacent local FC, thus making its way to the master FC. However, we ignore this possibility for the moment, keeping in mind that including this "macro diversity" will only improve the results.

Because of random access, packets may collide at the FC. Note that a collision between two packets is most likely to occur, while collisions of 3 or more packets can safely be neglected. Colliding packets originating

from sensors within the local FC's district, will be received at the same power level, and hence will both be lost in the collision. If, however, one of the interfering packets originated from the neighboring district, then the local packet's received power may still be stronger than the colliding packet's received power, resulting in the successful detection of the local packet. Let us define a tolerable level of interference to the desired signal by the threshold b, i.e., for a packet to be successfully received, the signal to noise and interference ratio (SINR) has to satisfy

$$\frac{P_T(r)/A(r,f_0)}{P_T(r')/A(2R-r',f_0)+\eta(f_0)B} \geq b \qquad (8)$$

where $P_T(r')$ is the interfering signal's transmit power and r' is the interfering node's distance to its FC, as shown in Fig. 2, and $b > 1$ is a constant. From Eq. (7), it follows that $P_T(r') = \gamma_0 A(r', f_0)\eta(f_0)B$, thus one can solve for the interference radius R_{int} from

$$\frac{A(2R-R_{\text{int}},f_0)}{A(R_{\text{int}},f_0)} = \frac{1}{b} - \frac{1}{\gamma_0} \qquad (9)$$

Note that choosing f_0 as the design point corresponds to the worst-case SINR, i.e., if condition (8) is satisfied for f_0, it will also be satisfied for any $f \in [f_0, f_0 + B]$.

For a given district radius R, a desired received SNR γ_0 and a threshold b, Fig. 3 shows the interference radius R_{int} vs. the operating frequency. We note that R_{int} decreases with the frequency; thus, operating at higher frequencies reduces the interference radius.

The interference radius R_{int} characterizes the area over which packet collisions result in packet loss. Hence the probability of successful packet detection can be determined as the probability that the arrival time of packets originating over the region of radius R_{int} do not overlap. This probability will be determined in Section III. Let us define N_1 as the number of nodes within the interference region, i.e.,

$$N_1 = \rho\pi R_{\text{int}}^2 = \frac{N}{D}c_R^2 \qquad (10)$$

where $c_R = R_{\text{int}}/R$. Fig. 4 shows c_R vs. the district radius R. As shown in the figure, c_R decreases with R, indicating that the interference becomes more pronounced as R gets smaller, or equivalently, as the number of districts grows. However, we note that this dependence is weak, i.e., c_R is almost constant.

III. Packet Collection Process

We assume that all local FCs are linked to a master FC via a flawless backbone. In order to recover the map of the field, the master FC requires $N_s = CS\log N$ *useful* packets, where S denotes the sparsity of the sensing field and C is a constant independent of N and S [1], [5]. Useful packets consist of those packets that are neither corrupted by interference, nor are repetitive [5]. If K_i denotes the number of useful packets collected by the ith local FC during one collection interval T, then the master FC collects a total $K = K_1 + K_2 + \ldots + K_D$ packets. We assume that each node generates packets according to independent Poisson processes at an average rate of λ_1 packet per second. The probability of successful reception is then the probability that packet transmissions originated within the interference region do not overlap,

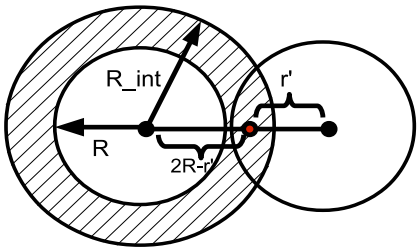

Fig. 2. The area characterized by R_{int} corresponds to the area over which packet collisions will result in packet loss. In other words, the transmission power of the sensors in the shaded area is strong enough to cause destructive (non-negligible) interference to the packets from the local FC's district.

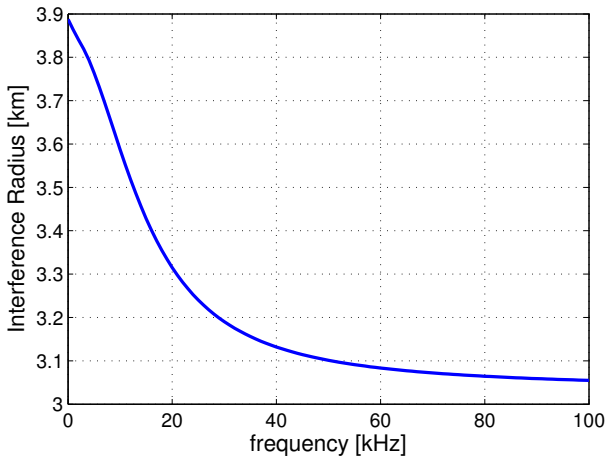

Fig. 3. Interference radius R_{int} plotted vs. the frequency, for $R = 3$ km, $b = 2$ and $\gamma_0 = 10$ dB.

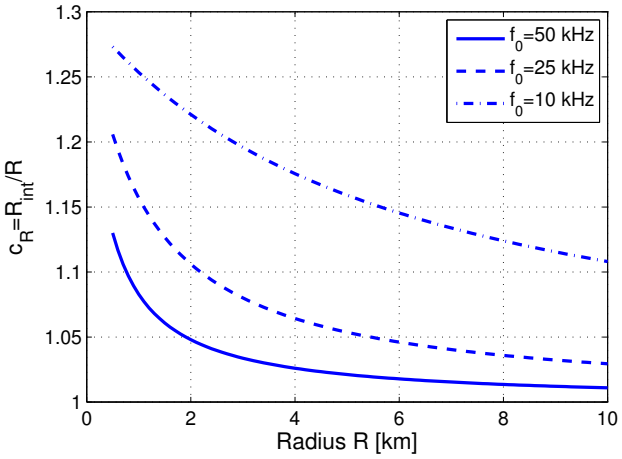

Fig. 4. $c_R = R_{\text{int}}/R$ plotted vs. the district radius R, for $b = 2$ and $\gamma_0 = 10$ dB.

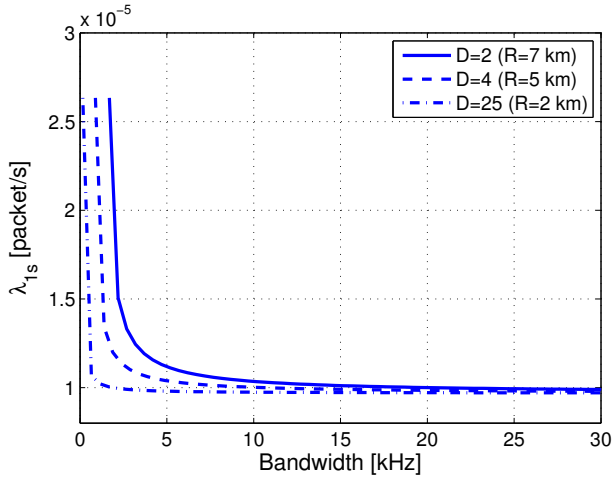

Fig. 5. λ_{1s} vs. bandwidth B for $f_0 = 10$ kHz, $S_{\text{tot}} = 314$ km^2, $N = 50 \times 10^3$ nodes, $\alpha_s = 482$ packets, $T = 1000$ s and $L = 1000$ bits per packet. The minimum per-node sensing rate decreases with the bandwidth B, as well as with the number of districts D.

i.e.,

$$p_c = e^{-2N_1\lambda_1 T_p} \tag{11}$$

where T_p is the packet duration, λ_1 is the sensing rate per node and N_1 is the number of nodes within the interference region as defined in Section II-B. The packet duration T_p depends on the system bandwidth B as $T_p = L/B$, where L, the number of bits per packet, is assumed to be fixed. The K_is are then modeled as independent Poisson processes with average arrival rates at the local FCs λ_0', given by [5]

$$\lambda_0' = \frac{N_0}{T}\left(1 - e^{-\lambda_1 T p_c}\right) \tag{12}$$

Now, the total packet arrival at the master FC can also be modeled as a Poisson process with an average rate given by

$$\lambda' = D\lambda_0' = \frac{N}{T}\left(1 - e^{-\lambda_1 T p_c}\right) \tag{13}$$

The design objective is to determine the minimum per-node sensing rate such that

$$\text{Prob}\{K = \sum_{i=1}^{D} K_i \geq N_s\} \geq P_s \tag{14}$$

which can also be expressed as demanding the average number of useful packets collected, $\alpha = \lambda' T$, to be greater than a target value α_s,

$$\alpha \geq \alpha_s \tag{15}$$

where α is given by

$$\alpha = N(1 - e^{-\lambda_1 T p_c}) \tag{16}$$

and α_s is the average number of useful packets required to ensure the sufficient sensing probability P_s is met.

Determining the minimum sensing rate employed by each sensor then follows closely from [5] and is given by

$$\lambda_{1s}(f_0, D) = \frac{-D}{2Nc_R^2 T_p} W_0\left(\frac{2NT_p c_R^2}{TD}\log\left(1 - \frac{\alpha_s}{N}\right)\right) \tag{17}$$

where $W_0(\cdot)$ is the principal branch of the Lambert W function. Note that c_R depends on the number of districts D (or equivalently, on the district radius R) as well as the operating frequency f_0, as was illustrated in Fig. 4.

Fig. 5 shows $\lambda_{1s}(f_0, D)$ vs. the bandwidth, for different D. As noted from the figure, the per-node sensing rate $\lambda_{1s}(f_0, D)$ decreases with the bandwidth. It also decreases as the number of districts grows. As we will see in Section V, a lower per-node sensing rate translates into lower energy consumption.

IV. Minimum Required Bandwidth

In order to meet a certain sufficient sensing probability P_s, a minimum bandwidth is required. This minimum bandwidth follows closely from [5] and is determined as

$$B_s(f_0, D) = \frac{2NLc_R^2 e}{TD}\log\left(\frac{1}{1 - \alpha_s/N}\right) \tag{18}$$

where L is the number of bits per packet.

Fig. 6(a) shows the minimum required bandwidth vs. the operating frequency f_0. We note that the minimum bandwidth reduces as the operating frequency f_0

increases; hence, for a bandwidth-limited system the desired operating frequency can be adjusted so as to allow for operation at lower bandwidths. Reducing the bandwidth requirement, however, may come at the price of a larger transmission energy, as will be explained in Section V. In Section VI, we will discuss how to choose the optimal operating frequency in accordance with the district size, so as to minimize the energy consumption.

The reduction in the minimum bandwidth that comes from employing a hierarchical structure, is given by

$$\frac{B_s(f_0,1)}{B_s(f_0,D)} = \frac{D}{c_R^2} \tag{19}$$

Fig. 6(b) shows B_s vs. the number of districts D, for a given operating frequency $f_0 = 10$ kHz. As illustrated in the figure, the bandwidth requirements can be lowered using a hierarchical structure. Lowering the bandwidth requirement is an attractive feature for networks with limited bandwidths, such as underwater acoustic networks. Hence, by dividing a large area into multiple districts, a hierarchical network structure not only benefits from reduced transmission energy (smaller transmission distance between sensors and their local FCs) but also from lower bandwidth requirements. This is not to say that one would operate at this minimum bandwidth B_s if more bandwidth is available. On the contrary, from an acoustic point of view, a smaller transmission distance enables the use of larger bandwidths, which in turn reduces the per-node sensing rate, as shown in Fig. 5. As we will see in Section V, a smaller λ_{1s} then reduces the energy consumption. Thus, from an energy point of view, it is desirable to use larger bandwidths, when available.

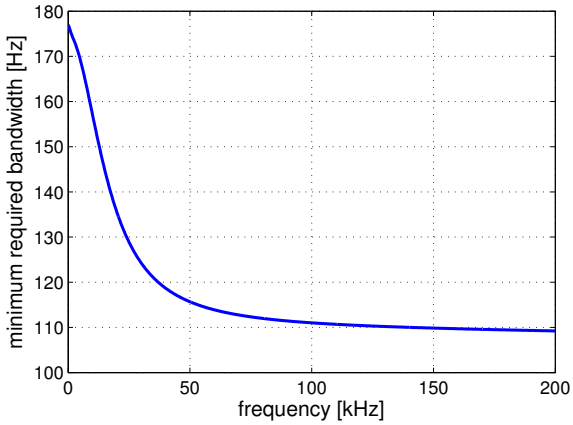

(a) Minimum required bandwidth B_s vs. operating frequency f_0, for $R = 2$ km.

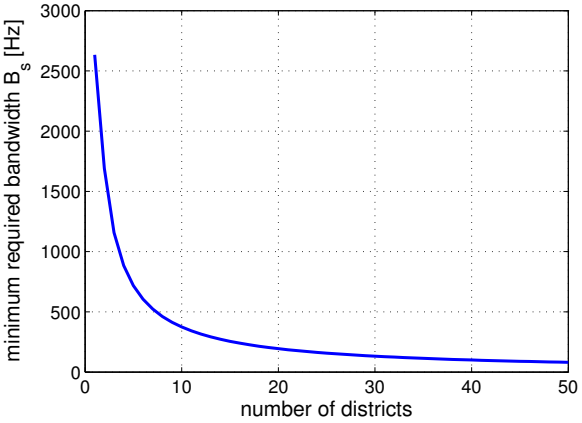

(b) Minimum required bandwidth B_s vs. number of districts D, for $f_0 = 10$ kHz.

Fig. 6. Minimum required bandwidth B_s decreases with both f_0 and D.

V. Transmission Energy

The total energy consumption in a hierarchical network consists of two components: i) the energy consumed to transmit data from the sensor nodes to the local FCs, and ii) the transmission energy used to convey the gathered data from the local FC to the master FC. The latter component is comprised of a fixed cost which depends on the geometry of the hierarchical structure and the relative position of the local FCs with respect to the master FC. Re-charging the sensor batteries in a large-scale network is often difficult, due to the sheer number of the nodes and the fact that they may be located in hard-to-reach areas. Hence, to extend the network lifetime, conserving the sensor nodes' battery supply is of utmost importance. The local FCs, however, are limited in number and could be re-charged more easily. In other words, the local FCs have more access to energy supply than the sensor nodes. Hence, the energy consumption by the sensor nodes poses the energy bottleneck, and determines the network lifetime. With this fact in mind, let us now examine the transmission energy required for data collection by the local FCs.

For a given bandwidth B, the transmission power at distance r is given by Eq. (7). The average per node transmission power is then given by

$$\begin{aligned}\overline{P_T} &= \int_0^R P_T(r)\frac{2\pi r\rho}{N_0}dr = \frac{2\gamma_0}{R^2}\eta(f_0)B\int_0^R A(r,f_0)rdr \\ &= \frac{2\gamma_0 A_0}{R^2}\eta(f_0)B\int_0^R a(f_0)^r r^{k+1}dr\end{aligned} \tag{20}$$

The above integral can be evaluated numerically.

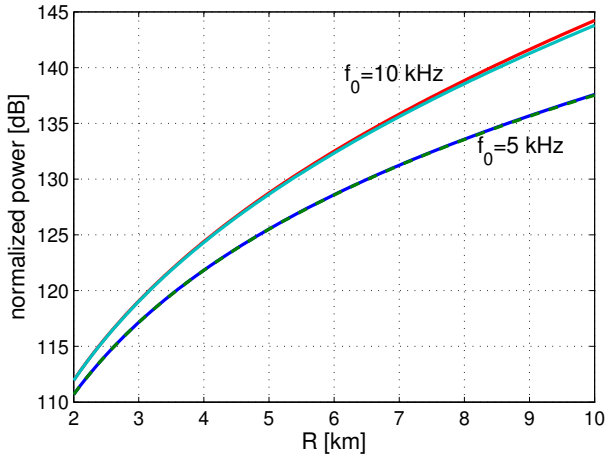

Fig. 7. Normalized power $\frac{\overline{P_T}}{2\gamma_0 A_0 \eta(f_0) B/R^2}$ vs. R for different f_0. The solid lines indicate the actual normalized power, whereas the dashed lines indicate the approximation. We note that the approximation is valid, especially for smaller f_0.

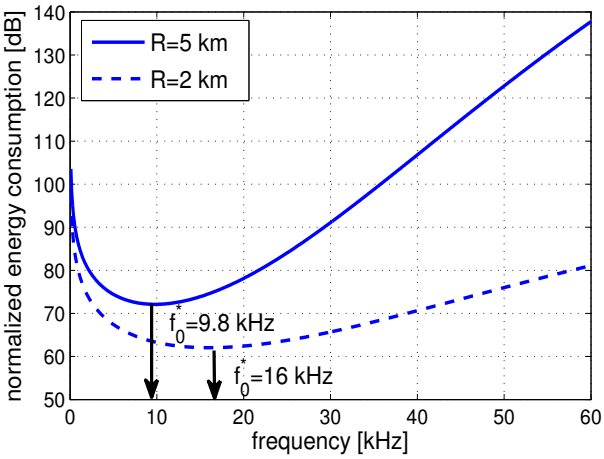

Fig. 8. Normalized energy consumption vs. the frequency, for $R = 2$ km and $R = 5$ km. The corresponding optimal operating frequency $f_0^\star$ is indicated in the figure.

To provide more insight into the power and energy consumption, one can also turn to an approximation. Noting that the absorption coefficient $a(f_0)$ is only slightly greater than 1, we can use the approximation $a(f_0)^r = (1+\epsilon_0)^r \approx 1 + r\epsilon_0$, resulting in

$$\overline{P_T} = 2\gamma_0 A_0 \frac{R^k}{k+2} \eta(f_0) B a(f_0)^{R\frac{k+2}{k+3}} \tag{21}$$

Fig. 7 examines the validity of this approximation by showing the normalized power from Eq. (20) and its approximate value from Eq. (21), for different f_0.

Assuming that the nodes transmit at the minimum rate λ_{1s}, the total average energy consumption of a hierarchical RACS network is given by

$$\overline{E}(f_0, B, D) = N\lambda_{1s}(f_0, D) T T_p \overline{P_T} \tag{22}$$

Using Eqs. (21) and (22), this energy is given by

$$\overline{E}(f_0, B, D) = 2NLT\lambda_{1s}(f_0, D)\gamma_0 A_0 \frac{R^k}{k+2} \eta(f_0) a(f_0)^{R\frac{k+2}{k+3}} \tag{23}$$

Note that the energy required for field reconstruction depends on a number of parameters: i) the number of districts D, which determines λ_{1s}, ii) the operating frequency f_0, which affects $\eta(f_0)$, $a(f_0)$ and, to a lesser degree, λ_{1s}, and iii) the bandwidth B which impacts the per-node sensing rate λ_{1s} (the higher the bandwidth, the lower the per-node sensing rate, as shown in Fig. 5).

VI. Resource allocation

In this section, we will determine the optimal operating frequency in accordance with the size of the district. For a given $B > B_s$ and a given D, the optimal operating frequency $f_0^\star$ is chosen as the frequency at which the energy consumption is minimized, i.e.,

$$f_0^\star = \arg\min_{f_0} \overline{E}(f_0, B, D) \tag{24}$$

An example is illustrated in Fig. 8, where the normalized energy consumption is plotted vs. the frequency (the energy $\overline{E}$ is normalized by $\frac{2NLT\gamma_0 A_0}{k+2}$). The optimal operating frequency then corresponds to the frequency $f_0^\star$ at which the energy consumption is minimal. Fig. 9 shows the optimal frequency vs. the number of districts D. The following parameters were used to generate the example figures: node density $\rho = 160$ nodes/km^2, sparsity $S = 20$, collection interval $T = 1000$ s, number of bits per packet $L = 1000$ bits, probability of sufficient sensing $Ps = 0.99$, $b = 2$, field size $S_{\text{tot}} = 314$ km^2, $\gamma_0 = 10$ dB and $B = 10$ kHz.

For a fixed f_0, the energy consumption scales with $\lambda_{1s}(f_0, D)$ and R, both of which are decreasing in the number of districts D. Fig. 10 compares the normalized energy consumption using optimal frequency assignment with that using fixed f_0 assignments. For a given number of districts D, by optimizing f_0 we can further reduce the energy consumption by considering the path-loss and noise functions. Hence, energy always decreases with the number of districts, but allocating f_0 optimally in accordance with the district size strikes an overall

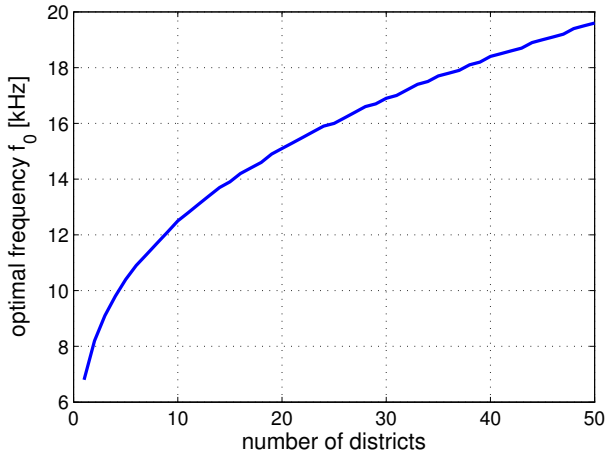

Fig. 9. Optimal operating frequency $f_0^\star(D)$ obtained from Eq. (24) plotted vs. the number of districts D. The following system parameters are used: $\rho = 160$ nodes/km^2, $S_{\text{tot}} = 314$ km^2, sparsity $S = 20$, $T = 1000$ sec, $L = 1000$ bits, $P_s = 0.99$, $b = 2$, $\gamma_0 = 10$ dB and $B = 10$ kHz.

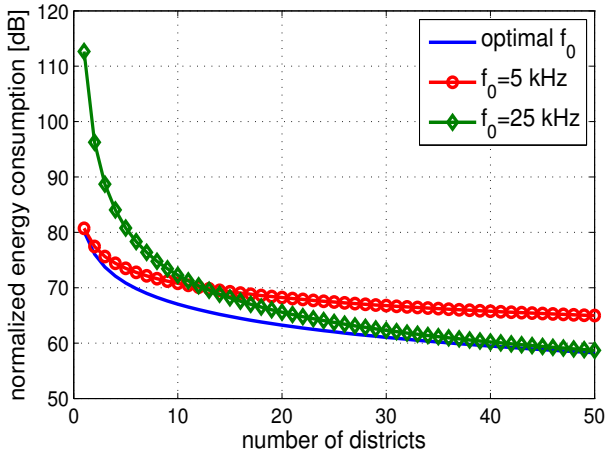

Fig. 10. Normalized energy consumption vs. the number of districts D. Allocating the frequency f_0 optimally in accordance with the district size minimizes the total energy consumption.

minimum.

Employing a hierarchical structure and optimally allocating the operating frequency, results in energy savings that can be quantified in dB as

$$G = 10 \log_{10} \frac{\overline{E}(f_0(1), B, 1)}{\overline{E}(f_0(D), B, D)} \tag{25}$$

Fig. 11 shows G vs. the number of districts D. The savings clearly increase as the number of districts grows. For example, for $D = 5$ we observe 10 dB reduction in the overall energy consumption of the network, compared to a non-hierarchical network. Shown in the

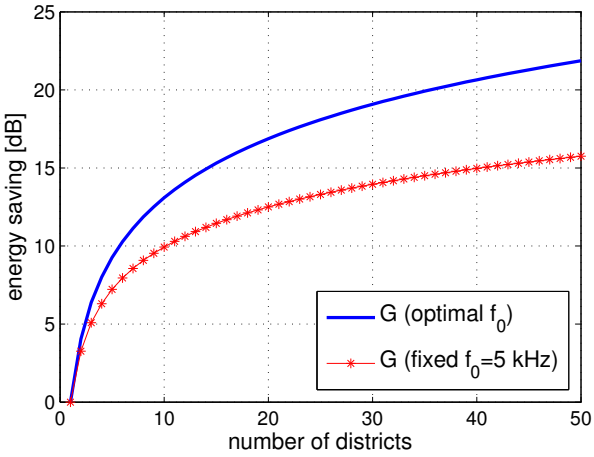

Fig. 11. Energy savings vs. the number of districts D.

figure is also the savings when the operating frequency is not optimally assigned but fixed at $f_0 = 5$ kHz. Optimal assignment of f_0 boosts the savings over fixed f_0 assignment. For example, with $D = 15$, the additional gain is 4 dB.

Fig. 11 also shows that there is an effect of diminishing returns with increasing the number of districts. For example, in going from a single district to $D = 15$ districts, the gain is 15 dB, while a further increase to $D = 30$ districts provides only 4 dB additional gain. With more districts, there are also the costs of adding new local FCs, pointing to an optimal number of districts D for a practical implementation..

VII. Conclusion

In this paper, we studied a hierarchical data collection scheme for an underwater acoustic network, using Random Access Compressed Sensing (RACS). We divided a large sensing field into D districts, where each district communicates its data to a local FC. The local FCs then transmit the collected packets to a master FC where recovery of the map of the sensing field occurs. Considerable energy savings are attained by employing a hierarchical structure. We showed that these savings are further enhanced by optimally allocating the operating frequency. We also showed that the minimum bandwidth requirements of a hierarchical network are reduced, compared to a single-district network. These features (lower bandwidth requirement and less energy consumption) are appealing for bandwidth and energy limited networks.

References

[1] F. Fazel, M. Fazel, and M. Stojanovic, "Random access compressed sensing for energy-efficient underwater sensor networks,"

IEEE Journal on Selected Areas in Communications (JSAC), vol. 29, no. 8, Sept. 2011.

[2] Q. Ling, G. Wu, and Z. Tian, "Collaborative environmental monitoring with hierarchical wireless sensor networks," *Environmental Monitoring*, pp. 461–476, November 2011.

[3] B. Sadler, "Fundamentals of energy-constrained sensor network systems," *Aerospace and Electronic Systems Magazine, IEEE*, vol. 20, no. 8, pp. 17 –35, Aug. 2005.

[4] J. M. J. Montana, M. Stojanovic, and M. Zorzi, "On joint frequency and power allocation in a cross-layer protocol for underwater acoustic networks," *IEEE Journal of Oceanic Engineering*, vol. 35, no. 4, pp. 936–947, October 2010.

[5] F. Fazel, M. Fazel, and M. Stojanovic, "Random access compressed sensing over fading and noisy communication channels," in *IEEE International Symposium on Information Theory Proceedings (ISIT)*, July 2012, pp. 1613 –1617.